Pure & Appl. Chem., Vol. 60, No. 5, pp. 769–780, 1988.
Printed in Great Britain.
© 1988 IUPAC

Diagnostics and control of low pressure plasmas for the chemical vapor deposition (CVD) of amorphous semiconductor and insulator films

Kunihide Tachibana

Department of Electronics, Kyoto Institute of Technology,
Matsugasaki, Sakyo-ku, Kyoto 606, Japan

Abstract - Recent developments in the diagnostics of low pressure plasmas for the CVD of amorphous semiconductor and insulator films are reviewed. Stress is placed on the analyses of the temporarily and spatially varying plasma structure and plasma parameters and the reaction kinetics in the gas-phase and on the solid surface. Under the knowledge of these characteristics of the CVD plasmas, some means for controlling the plasmas are discussed and examples tried recently in Japan for the preparation of good quality a-Si:H and Si-containing alloys or compounds are introduced.

INTRODUCTION

Low pressure non-thermal plasmas, in which the electron temperature is much higher than the gas temperature, have been successfully used for the chemical vapor deposition of various electronic and optical materials such as amorphous silicon and its compounds. The most important role of the plasma is to initiate the decomposition of source gas molecules like a powerful hammer utilizing the high electron energy producing chemically reactive species for the deposition. However, we may become aware that there are so many other roles played by the plasma in the CVD process; (a) secondary homogeneous (gas phase) reactions in which the primarily produced ions and radicals change their relative abundances or produce new kinds of ions and radicals, (b) transportation of the ions and radicals produced in the plasma to the substrate surfaces and (c) initiation of the surface reactions for the deposition of the films. All of these roles must be controlled carefully in order to prepare films of desired compositions and properties.

Since 1985 we have organized a group in Japan under the name of "Plasma Electronics Society", and have been holding a Symposium on Plasma Processing every year for a systematic study of the characteristic properties of such non-equilibrium plasmas. Our aim is to clarify the relations of the external controlling parameters such as gas species, pressure, flow rate, input electric power, frequency and dimensions of the apparatus with the spatially and temporarily varying internal plasma parameters such as electric potential or field strength, electron temperature or energy and the density. On the basis of these systematic investigations we believe that we can understand the roles of plasmas in the CVD processes and can give guiding principles to the finer control of the plasmas for any desired purposes.

In this talk we will review mainly the present status of activities of our group for the diagnostics and control of the low pressure plasmas restricting ourselves to the field related to the CVD of amorphous silicon and its compounds. This has a purpose of introducing some of our latest results which have been published in the proceedings of our conference written in Japanese. However, some interesting results published in foreign countries will also be reviewed, from which the members of our group must learn and get hints for the future developments.

INITIAL PROCESSES

Potential distribution and EEDF in plasma—theoretical analysis

Let us consider a typical diode type apparatus equipped with parallel plane electrodes. When it is powered by an RF generator through a DC-blocking capacitor, an electric potential distribution across the electrodes is formed to sustain the discharge and to balance the net currents for electrons and for ions to the both electrodes. Temporal and spatial variations of this potential, or the electric field strength given by the gradient of the potential, govern the electron and ion energy distribution functions and their densities in the plasma. This in turn affects probabilities of the electron collision events such as the decomposition, the excitation and the ionization of source molecules. Especially the structure of the sheath near the electrodes where ionic space charge is formed is important because it determines the extraction fluxes of ions due to drift and neutrals due to diffusion to the substrate and the energy of ions impinging upon the substrate. Therefore, much atten-

tion has been paid for the systematic analyses of this plasma structure (refs.1-4).

Theoretical approach for analyzing the potential distribution is usually based on the coupled equations composed of the Poisson's equation, the continuity equations for electrons and ions and the energy and momentum conservation equations. However, it is difficult to solve the coupled equations directly, so that in a specific model some simplifying assumptions are usually made, which restrict the generality of the model. A continuum model was developed by Graves and Jensen (ref.1) for an RF discharge in a diode type reactor, where the mean free paths of electrons and ions are assumed to be much smaller than the characteristic length such as the sheath thickness. This model is very interesting because it shows clearly the dynamic behaviors of the potential and electric field strength distributions, the electron and ion densities and the probability distributions for electron collision events over a cycle of the RF discharge. Many other models, on the other hand, assume the collisionless sheath (refs.2-4). However, in a typical plasma used for the CVD of amorphous silicon and its compounds the situation lies between the two extreme conditions.

Ichikawa <u>et al.</u>(ref.5) have reported a simplified sheath model under the following assumptions: the electric field strength is divided into the DC component E_{DC} and the RF component E_{RF}, $E = E_{DC} + E_{RF}\cos(\omega t)$; positive ions can not respond to the RF frequency; the ionization within the sheath region is negligible. The resulting equations becomes

$$\frac{dE_{DC}}{dx} = \frac{e}{\varepsilon_0} n_i , \tag{1}$$

$$j_e = - n_e \mu_e E - D_e \frac{dn_e}{dx} , \tag{2}$$

$$j_i = n_i \mu_i E_{DC} = J_0 , \tag{3}$$

$$\frac{dj_e}{dx} = \frac{dj_i}{dx} = 0 , \tag{4}$$

where n_e, j_e and μ_e are respectively the density, the flux and the mobility for electrons, n_i, j_i and μ_i are those for ions and D_e is the diffusion coefficient for electrons. Here, they imposed a condition that the electron and ion fluxes must be equal over one RF cycle;

$$\frac{1}{T}\int_0^T j_e \, dt = J_0 . \tag{5}$$

Then, the DC component of the electric field strength is given by

$$E_{DC}(x) = \left(\frac{2e}{\varepsilon_0}\frac{J_0}{\mu_i} x + C\right)^{1/2} , \tag{6}$$

where C is an integration constant. The equation for the electron density becomes

$$\frac{d^2n_e}{dx^2} + \frac{\mu_e}{D_e} E \frac{dn_e}{dx} + \frac{e}{\varepsilon_0}\frac{J_0}{\mu_i}\frac{\mu_e}{D_e}\left(\frac{2e}{\varepsilon_0}\frac{J_0}{\mu_i} x + C\right)^{-1/2} n_e = 0 . \tag{7}$$

Using the obtained n_e over one cycle, J_0, C and E_{RF} are determined by eq.(5). An example of the results for E_{DC} and n_i is shown in Fig.1 where $J_0 = 7.5 \times 10^{13}$ $cm^{-2}s^{-1}$, $E_{DC}(x=0) = 30$ Vcm^{-1} are given as initial conditions.

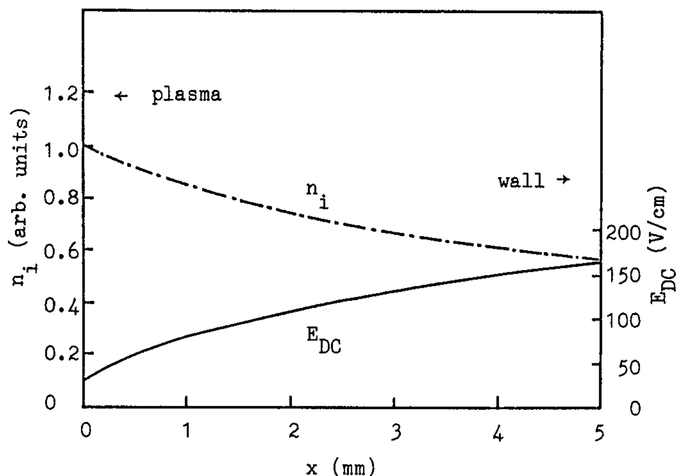

Fig.1. Calculated spatial distributions of the electric field strength E_{DC} and the ion density n_i. $C^{1/2}$ was determined to be 30 Vcm^{-1} (ref.5).

Tagashira <u>et al.</u>(ref.6) have modeled the RF discharge using a Monte Carlo simulation technique similar to the one developed by Kushner (ref.7). In their treatment, however, the temporal change of the sheath thickness L_s is considered by assuming a constant gradient m of the electric field in the sheath as follows:

$$m = 2(V_{sDC} + V_{RF}/2)/(L_s(max))^2, \tag{8}$$

$$L_s = (2V_s/m)^{1/2}, \tag{9}$$

where V_{RF} is the applied RF voltage, V_{sDC} is the DC self-bias voltage

determined in the calculation by the balance of electron productions and losses, and V_s is the sheath voltage given by $V_s = V_{sDC} + V_{RF}\cos(\omega t)$. Their typical result for the spatial dependent excitation events in a nitrogen plasma is shown in Fig 2. Comparing the result with a simulation with fixed sheath thickness like the earlier work of Kushner (ref.7), their treatment produces more realistic results which can explain the experimental observation. The effect of wave-riding electrons powered by the movement of the sheath edge and transported into the bulk plasma is reflected on the distribution.

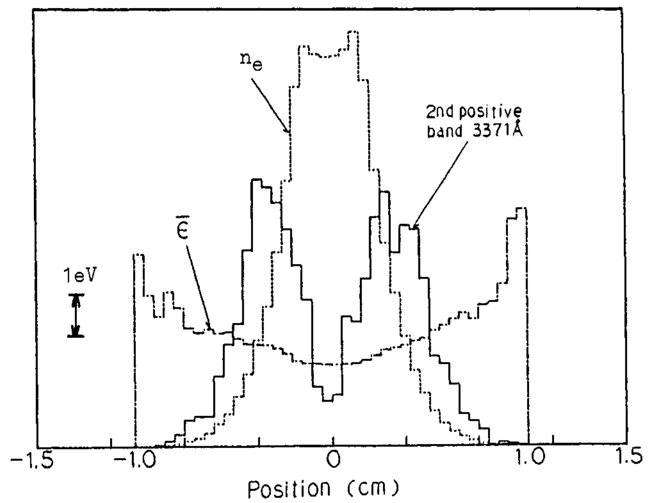

Fig.2. Spatial distributions of the mean electron energy , the electron density n_e and the emission intensity of 2nd positive band in an N_2 plasma at V_{RF} = 60 V, p = 0.5 Torr and $L_s(max)$ = 0.9 cm (ref.6).

The electron energy distribution function (EEDF) has been calculated by the Monte Calro simulation and the spatial and temporal behavior has been discussed(ref.8). Using the Boltzmann equation analysis, Makabe et al.(ref.9) has calculated the change in the EEDF as a function of the RF frequency ω and found that the average electron energy decreases as ω becomes larger than the electron collision frequency ν_e. Mase et al.(ref.10) analyzed the conditions for sustaining the discharge by the continuity relation of plasma density and the energy balance equation, and found a simple relation between the electric input power P, the plasma density n and the sheath thickness L_s;

$$n^2 = (\varepsilon_0 \pi / e^2 \omega)(P / L_s^3) . \qquad (10)$$

Itatani (ref.11) tried to formulate the conditions for sheath formation in a plasma which contained negative ions at a density n^- using relations similar to the Bohm criterion considering a transition region between the plasma and the sheath. He has concluded that the potential energy at the edge of the transition η_s must fulfill the conditions

$$\eta_s > (1/2)[1 + (\gamma - 1)\alpha_s]^{-1} , \qquad (11)$$

$$\eta_s^2 < (3/4)[1 + (\gamma^2 - 1)\alpha_s]^{-1} , \qquad (12)$$

where γ is the ratio of the electron temperature T_e to the negative ion temperature T_n and α_s is given by the value of $n^-/(n^- + n_e)$ at the sheath edge. These two conditions never cross with each other and a stable sheath is formed when γ is within the region

$$5 - \sqrt{24} < \gamma < 5 + \sqrt{24} . \qquad (13)$$

Outside this region the plasma can take one of the two different sheath structures as follows. An example of the calculated results at γ = 20 is shown in Fig. 3 for relations of η_s with α_s calculated at boundaries given by eqs.(11) and (12) together with the relations of η_s with α, which is given by the value of $n^-/(n^- + n_e)$ in the bulk plasma, obtained by

$$\alpha = \alpha_s \exp(-\eta_s)/[\alpha_s \exp(-\eta_s) + (1 - \alpha_s)\exp(-\gamma\eta_s)] . \qquad (14)$$

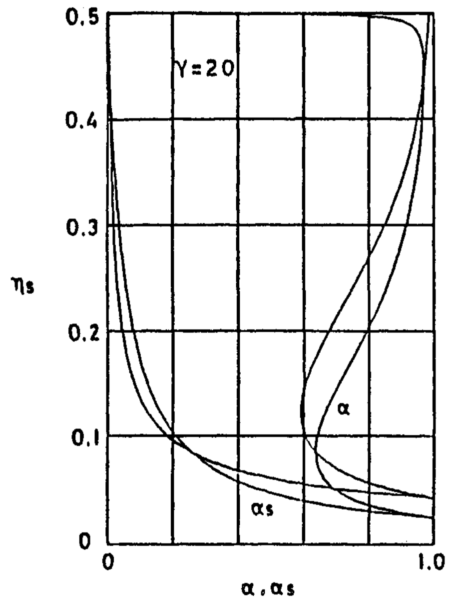

Fig.3. Relations of η_s vs α_s and η_s vs α calculated at boundaries given by (11) and (12) for γ=20. Two curves for η_s vs α_s cross at (α_s, η_s) = (0.256, 0.085) and (0.007,0.440). The corresponding values of α become 0.635 and 0.969, respectively (ref.11).

From this figure we can see that there is a region where three different values of η_s correspond to a value of α, while one of the η_s's (middle value) can

not be realistic because the calculated electric field becomes imaginary.

Another interesting behavior, i.e., plasma instability, is suggested by Suganomata *et al.* (ref.12) in a plasma including negative ions.

Potential distribution and EEDF in plasma—measurement

Most convenient method for the measurement of potential or electric field distribution across the electrodes is to use an electro-static probe. However, many problems arise inherent to the RF discharges for CVD. Some of the most important problems which have been discussed are as follows; (a) a problem caused by the rectifying current due to the non-linear probe characteristics to the fluctuating RF potential(ref.13), (b) a problem caused by the probe surface contamination due to the film deposition (ref.14), and (c) a problem due to the presence of negative ions (ref.15).

Sugawara *et al.*(ref.16) measured the time averaged potential distribution in a diode type reactor using a shielded single-probe in an argon plasma. Their result for the DC sheath voltage shows that V_{sDC} remains constant below p = 0.3 Torr but starts to drop as p becomes higher according to $p^{-2/3}$. They measured also the spatial dependence of the time varying component of the potential v_{RF} using an capacitive probe. Typical results are shown in Fig.4 as a function of position normalized by the sheath thickness.

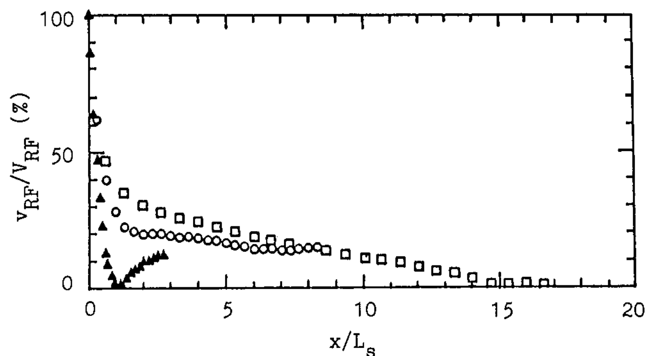

Fig.4. Time varying component of the electric potential v_{RF} normalized by the applied RF voltage V_{RF} as a function of the distance x from the cathode normalized by the sheath thickness L_s at an RF power of 15 W and at some values of the gas pressure: □,1; ○,0.1; △,0.01 Torr (ref.16).

Sato *et al.*(ref.17) proposed that the time varying potential and electric field strength in an RF plasma could be measured from the probe characteristics by a simple analysis similar to the theory of Boschi *et al.*(ref.18) They measured the probe characteristics in their specially designed apparatus in which they could produce either the time varying space potential or the time varying electric field depending on the position. A typical characteristics is shown in Fig.5 where they claim that the distance between the two deflecting points corresponds to the amplitude of the varying potential. The value of the electron saturation current I_{es} was time varying, when it was measured at a position where only the variation of the electric field strength existed; $E_0(t) = E_0\cos(\omega t)$. The difference of the values at ωt = 0 and $\pi/2$ is given by

$$I_{es}(\omega t=\pi/2) = [2 - \cos(a_e)]I_{es}(\omega t=0), \qquad (15)$$

where $a_e = eE_0/m\omega v_{th}$, and v_{th} is the thermal velocity of electrons. From this relation the electric field strength can be deduced.

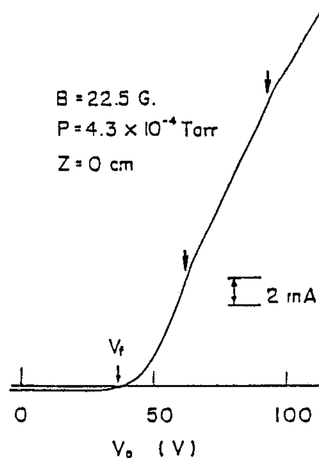

Fig.5. Example of the time averaged probe characteristics measured at p = 4.3 x 10^{-4} Torr. Arrows show the deflection points described in the text (ref.17).

Another interesting method for the measurement of local electric field strength is to use the laser induced fluorescence (LIF) such as performed by Gottscho *et al.*(ref.19) in a BCl_3 plasma for etching, where the Stark effect on a band spectrum of BCl has been utilized. A similar way has ever been tried by Oda *et al.*(ref.20) in a theta-pinch plasma where a He forbidden line has been used. However, detection sensitivity in the experiment of Gottscho *et al.* was higher because of the larger Stark effect. Some methods suitable for the CVD plasma in such gases as silane and methane must be developed as a non-disturbing electric-field measurement.

Electron impact dissociation of source gas molecules

Since electron impact dissociations and ionizations are the primary processes in the CVD, much research has been stimulated and basic data have been compiled recently for many commonly used gases such as CH_4, SiH_4 and so on. Goto *et al.* have been performing a series of measurements of the effective emission cross sections for electron collisions producing some

of the electronically excited states of Si and SiH in SiH_4(ref.21), NH in NH_3 (ref.22) and Ge and GeH in GeH_4(ref.23), respectively, by an electron beam experiment. Recently they established a delayed-coincidence photon-counting method and deduced the level excitation cross section for some of the Si·atomic levels by eliminating the cascade effects from higher lying levels (ref.24). On the other hand, dissociation processes in which neutral species are produced in their ground states are quite difficult because the detection of non-light-emitting radicals is not simple, especially when the densities are low, as will be mentioned in the next section.

Using a Boltzmann analysis Tagashira et al. derived recommended sets of cross sections for electron collisions with SiH_4(ref.25) and CH_4(ref.26), with which they could reproduce swarm parameters consistent with the measured ionization and attachment coefficients.

Detection of the dissociation degree of source gases

As a first step to the understanding of the CVD plasmas the dissociation degrees of the source gases have to be measured. Tachibana et al.(refs.27,28) have developed a laser absorption method using a He-Ne laser(3.39 µm) for CH_4 and CO_2 laser(10.59 µm) for SiH_4 for in situ monitoring of the partial pressures of the parent gases under the CVD condition. They investigated the dissociation degree of CH_4 and SiH_4 as functions of the external parameters such as the RF power, the gas flow rate and the gas pressure. They also studied the dissociation rate constant, which means the product of dissociation rate constant and electron density, from the speed of the initial decay of the source gases in a sealed-off system.

Hata et al.(ref.29) have used a coherent antistokes Raman spectroscopy (CARS) method and measured the temporal and spatial variation of the source gas densities in the plasma of SiH_4, Si_2H_6 and GeH_4. A typical result is shown in Fig.6 where the density distribution of SiH_4 between the electrodes is shown together with the result of LIF measurements of Si. They also observed in a silane plasma a slight increase of H_2 density near the electrode surface from which the elimination of H_2 from the surface was suggested (ref.30).

GAS-PHASE REACTIONS

Detection of ions and radicals in the plasma

Primarily produced ions and radicals, for example SiH_n^+ and SiH_n (n=0-3) in silane plasma, and other fragments such as H and H_2 perform further reactions in the gas-phase where they change their relative densities or produce new ionic and neutral species before reaching the substrate surface. Therefore, the identification and the quantitative detection of the chemically reactive species are very important for understanding the plasma chemistry in the CVD processes. Recently much attention has been paid to the non-perturbing spectroscopic methods such as OES(optical emission spectroscopy), LIF and CARS.

Tachibana et al.(ref.31) detected Si atom by a conventional line absorption technique in a SiH_4(5%)-Ar plasma produced by an RF discharge in a diode type reactor, where the density reached to the order of 10^{10} cm^{-3}. But in a plasma of SiH_4(10%)-H_2, which is preferable for better quality of the deposited film, the same method failed in the detection, suggesting that the density was lower than about 10^9 cm^{-3}. After the introduction of the LIF method as a diagnostics tool, Si atom has been successfully detected in various types of discharges for the CVD of a-Si:H. Takubo et al.(ref.32) have measured the spatial distribution of Si atoms in a DC discharge and in an RF discharge as well. Their result shows a density peak just in front of the substrate surface implying an evidence of the spattering of Si atoms from the substrate.

Inoue et al.(ref.33,34) have applied the LIF method to the detection of SiH_2 produced by the photodissociation of phenylsilane and measured the quenching rate constant of SiH_2 in various

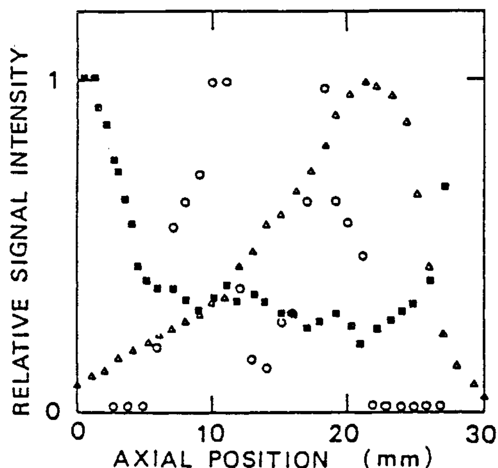

Fig.6. Spatial distributions of SiH_4 (■) measured by CARS, Si(○) by LIF and Si* (△) by OES in an RF plasma of 100% SiH_4 at a pressure of 0.1 Torr, a flow rate of 10 standard cm^3min^{-1} and an RF power of 5 W (ref.29).

TABLE 1. Quenching rate constants for $SiH_2(X^1A_1)$ and for $CH_2(a^1A_1)$ measured in various gases at room temperature in units of $cm^{-3}s^{-1}$ (ref.34).

	$SiH_2(X^1A_1)$	$CH_2(a^1A_1)$
H_2	1.0±0.4(10^{-13})	1.3±0.1(10^{-10})
CH_4	1.0±0.3(10^{-12})	7.3±0.6(10^{-11})
SiH_4	1.1±0.2(10^{-10})	2.4±0.4(10^{-10})
Si_2H_6	5.7±0.2(10^{-10})	-----

gases. Their results are shown in Table 1 in comparison with the reported results for CH_2. They tried the detection of SiH_2 in a CVD plasma but were unsuccessful due to the background emission from the plasma.

Hirota et al. have established a method for the detection of $\dot{C}H_3$(ref.35) and SiH_3(ref.36) by an absorption method with a tunable infrared diode-laser. Application of the method to a real CVD plasma is expected. A problem common to the absorption and LIF methods at present is the lack of spectroscopic data such as the absorption oscillator strength for the derivation of absolute densities from the observed signals. Theoretical and experimental studies of such basic data are also required.

Matsumi et al.(ref.37) have detected Si, SiH and SiH_2 in a diode type CVD system by LIF. They measured the spatial distribution of these radicals. Moreover, they studied the RF power dependence of the densities in comparison with the results of OES where only the light-emitting excited species were monitored, and found an evidence that Si, SiH and SiH_2 are produced by electron collisions in one step. A decreasing tendency similar to the deposition rate was observed for the densities of the SiH_n(n=0-2) as the gas pressure increases. This suggests that the contribution of these radicals in the deposition is not negligible because the density of other presumably predominant radicals such as SiH_3 may increase as the pressure increases.

Another interesting method for the detection of ions and radicals is the mass spectrometry. This method has been applied by many authors to the detection of the ionic species in the real CVD situations (refs.38,39). Gallagher et al.(ref.40) applied this method to the detection of the neutral radicals in a DC proximity discharge in silane by using a threshold ionization technique. The principle is based on the small difference in the energies required for the direct ionization of radicals and for the dissociative ionization of the residual parent molecules by a few eV. According to their result the most predominant species in the silane plasma is SiH_3 and the densities of the aggregated radicals such as Si_2H_m reach nearly the same amount depending on the pressure, but the densities of Si, SiH and SiH_2 are usually much smaller than that of SiH_3.

A multi-photon ionization (MPI) method is also interesting when it is combined with a mass spectrometry. CH_3 radicals have ever been detected by this method (ref.41). Recently SiH_3 was detected by photo-ionization with VUV light source and the threshold ionization potential for SiH_3 was found to be 8.01 eV compared to the 12.086 eV for production of SiH_3^+ from SiH_4(ref.42).

Simulation of the gas-phase reactions

Under the compilation of the experimentally and theoretically obtained rate constants for various reaction processes of ions and radicals, simulation techniques for the gas-phase reactions have been developed. For a methane plasma used for the CVD of a-C:H Tachibana et al.(ref.27) calculated the dissociation degree of CH_4 using the electron-collision decomposition rates measured by their laser absorption method. They calculated also the densities of ions, radicals and stable molecules produced in the plasma as a function of the RF power. According to their estimation the most predominant radical is CH_3, but CH_2 and CH can also contribute to the deposition if the sticking probability of CH_3 is small. A large amount of H atoms produced in the plasma is expected to contribute to the surface reactions that eliminate hydrogen from the surface and promote C-C bondings.

For simulations of SiH_4 plasma used for the CVD of a-Si:H, there are less reaction data than for CH_4 available at present. Tachibana et al.(refs.43-45) have

TABLE 2. Examples of gas-phase reactions and the parameters A and E for the rate constants as given by $K = A\exp(-E/RT)\ cm^3mol^{-1}s^{-1}$, where R is the gas constant and T is the gas temperature. Numbers in ( ) mean the power of 10 by which each entries must be multiplied.

Reactios							A	E/R
H	+	SiH_4	→	SiH_3	+	H_2	3.6(13)	1250
Si	+	SiH_4	→	Si_2H_2	+	H_2	4.5(12)	0
SiH	+	SiH_4	→	Si_2H_5			5.6(13)	1000
SiH_2	+	SiH_4	→	Si_2H_6			2.1(12)	1000
SiH_2	+	SiH_4	→	Si_2H_4	+	H_2	7.2(12)	3000
H	+	Si_2H_6	→	SiH_4	+	SiH_3	1.0(14)	1500
H	+	Si_2H_6	→	Si_2H_5	+	H_2	2.0(14)	1500
SiH_2	+	Si_2H_6	→	Si_3H_8			3.7(13)	2000
Si_2H_4	+	SiH_4	→	Si_3H_8			2.7(13)	2000
Si_2H_4	+	Si_2H_6	→	Si_4H_{10}			2.0(13)	2000
H	+	Si_3H_8	→	Si_2H_6	+	SiH_3	1.0(14)	1500
H	+	Si_4H_{10}	→	Si_2H_6	+	Si_2H_5	2.0(14)	1250
SiH_3	+	SiH_3	→	SiH_4	+	SiH_2	1.8(13)	0
SiH_3	+	SiH_3	→	Si_2H_4	+	H_2	1.2(12)	0
Si_2H_5	+	Si_2H_5	→	Si_2H_6	+	Si_2H_4	1.0(13)	0
H	+	Si_3H_8	→	Si_2H_6	+	SiH_3	1.0(14)	1500
SiH_2	+	Si_3H_8	→	Si_4H_6			3.4(13)	2000

started to compile a self-consistent set of reaction data for SiH_4. In order to check the validity of the compiled data for reaction kinetics, they have tried two kinds of simulations; one for a thermal CVD system where SiH_2 is assumed to be the predominant primary radical (ref.44) and the other for a Hg-photosensitized CVD where SiH_3 is predominant (ref.45). The calculated results in both cases explain the measured depletion rate of SiH_4 and time evolution of reaction products such as Si_2H_6, Si_3H_8 and H_2. The main part of the compiled set is listed in Table 2.

Recently similar calculations have been performed by many authors for CH_4 plasmas (see, e.g., ref.46) and for SiH_4 plasmas (see, e.g., ref.47). The result of Kushner (ref.47) for a SiH_4 plasma shown in Fig.7 is very interesting because it qualitatively represents typical features of previously reported experimental results (refs.37,40).

Makabe et al.(ref.48) have built up a simple model for a silane discharge in a coaxial cylindrical reactor, which consists of the basic discharge equations and the Boltzmann equation for EEDF. They simulated the deposition rate of a-Si:H and the efficiency of gas utilization taking into account the effects of negative ions.

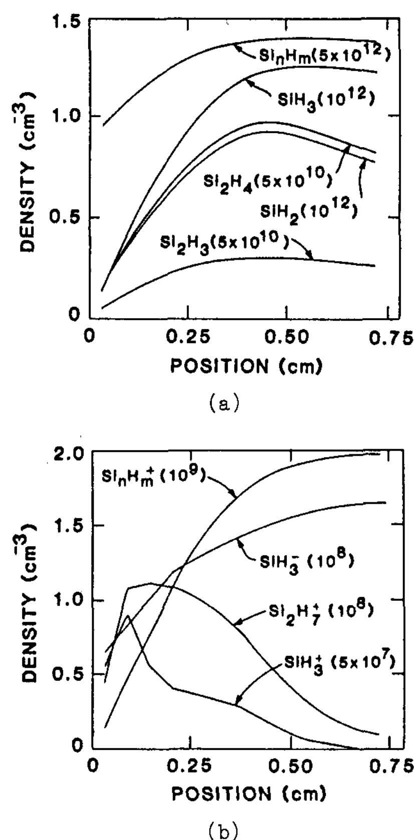

Fig.7. Calculated radical (a) and ion (b) densities in a discharge of 0.5 Torr SiH_4 at 50 $mWcm^{-3}$. The electrode is at x=0 and the midplane is at x=0.75 cm. The numbers in ( ) are multiplication factors for the vertical scale (ref.47).

TRANSPORT AND SURFACE REACTIONS OF IONS AND RADICALS

Transport of ions and neutral radicals to the substrate

The growth rate of deposited film is mainly determined by the flux of neutral radicals from the plasma to the substrate, although the quality of the film is affected by the ion flux. The neutral radical transportation is governed by the diffusion due to the density gradient near the substrate surface when the continuum approximation holds. Therefore, the measurements of density profiles of important neutral radicals have been tried by many authors (refs.29,32,37).

Takubo et al.(ref.32) measured the density of Si atoms by LIF in a DC discharge. If we estimate the Si atom flux from the maximum density of 4×10^8 cm^{-3} at a distance 3 mm from the cathode using a reported diffusion coefficient (ref.31), it becomes about 5×10^{11} $cm^{-2}s^{-1}$, which is lower than the total radical flux estimated from the deposition rate by about three orders of magnitude. Matsumi et al.(ref.37) also measured the spatial distribution of Si, SiH and SiH_2 by LIF in a conventional diode type RF discharge. However, they did not deduce the absolute densities of the radicals.

Some part of the transported radicals to the substrate is incorporated into the substrate but other part is reflected back into the plasma. Here we define the sticking probability β as the ratio of the part contributing to the deposition to the total incoming flux of a specific radical. If β is less than unity, it is reflected in the spatial distribution of radicals through the boundary condition for the density N at the substrate surface x_0 (ref.49);

$$N(x_0) = \left|\frac{dN(x)}{dx}\right|_{x=x_0} \left(\frac{2\lambda}{3}\right)\left(\frac{2-\beta}{\beta}\right) , \quad (16)$$

where λ is the mean free path of the radical. The absolute radical density in the plasma also becomes high if β is much less than unity and affects the total gas-phase reaction scheme . It is worth while noting the result in the measurement of the spatial distribution of O atoms in an oxygen plasma by Selwyn (ref.50), in which is shown clearly the dependence of the reactivity of O atoms on the substrate materials.

In a silane plasma the effective sticking probability for the total incoming flux was estimated by Schmitt et al.(ref.51) to be about 0.7, using a fine grid placed at a short distance (less than the mean free path) from the substrate. However, similar measurement in a Hg-photosensitized CVD by Perrin et al. (ref.52) predicted a value of about 0.1. In the latter case the predominant depositing radical is SiH_3, while in the former case other radicals such as SiH_2, SiH and aggregated Si-containing radicals may contribute to the deposition for which the sticking probability is considered to be nearly unity.

Recently Muraoka et al. (ref.53) measured the density of H atoms in a cylindrical DC discharge in hydrogen by LIF at a wavelength of L_α(121.6 nm). From the balance equations for H atoms in the plasma they estimated a loss probability of 6.7 x 10^{-3} at the Pyrex glass surface due to the recombination forming H_2. This kind of measurement must be interesting for a typical CVD plasma in a diode type reactor because the reactivity of H atoms must be quite different on the growing a-Si:H surface.

In a simulation of the gas-phase reactions in silane plasma Kushner has calculated the flux of various kinds of radicals as shown in Fig.8 (ref.47). It is seen from the figure that the compositions of the flux differ by the kinds of gas mixtures.

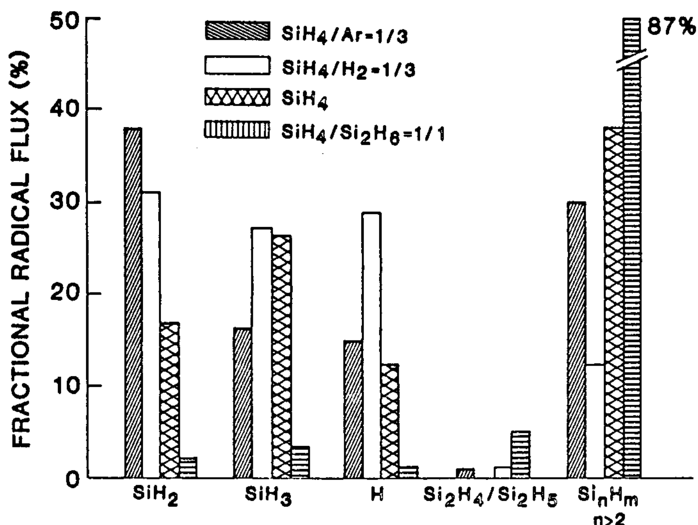

Fig.8. Fractional radical fluxes for discharges at a pressure of 0.5 Torr and an RF power of 10 mW cm^{-3} calculated for various gas mixtures (ref.47).

Surface reactions and film growth

Some surface reaction models have been proposed for the explanation of the deposition processes of a-Si:H in silane plasma (refs.54-56). Recently Kushner (ref.47) demonstrated a phenomenological model for a description of the surface reactions in which seven types species were taken into account: (1) gas-phase radicals which are fluxes onto the surface; (2) immobile adsorbed radicals; (3) mobile adsorbed radicals; (4) desorbed gas-phase molecules; (5) active surface sites; (6) silicon atoms bonded to the lattice but still on the surface; (7) silicon atoms incorporated into the film and buried beneath the surface. By this model he deduced not only the deposition rate but also the H-content and the H-bonding types in the deposited film. Calculated results can explain reported experimental results fairly well without any normalization parameters other than the sticking probability of Si_nH_m(n>2) which has been adjusted to 0.07.

Gallagher (ref.56) proposed a surface reaction model for SiH_3 considering some types of structures of a-Si:H surface. Tsuda et al.(ref.57) explained by a quantum chemical calculation a mechanism for the formation of diamond structure by a CH_3^+ ion on the $-CH_3$ covered surface or by a neutral CH_3 radical on the charged surface of the same kind.

On the experimental side there are no direct measurement of individual reactions on the growing surfaces. However, the effects of impinging ions onto the surfaces have been investigated by many authors. Matsuda et al. (ref.58) studied the effect of ions in the formation of micro-crystal structures in a-Si:H films and concluded that ion collisions at high energy led to destruction of the micro-crystal structure. Sugai et al.(ref.59) studied the ion collision effects on the H-bonding structure using a magnetic deflection method for removing impinging ions and obtained a conclusion that the bombardment of H^+ ions reduced the >Si-H_2 bonds but increased -Si-H bonds. Tagashira et al.(ref.60) showed in an AC discharge at 50 Hz for the deposition of a-SiN:H films that the secondary electron emission by ion collision helped sustenance of the discharge, while no damages like pin holes were produced by the ion collisions.

Hirose et al.(ref.61) tried to extract the radicals from the plasma into an ultra high vacuum chamber where a substrate was held. In their experiment a lower temperature epitaxial-growth of Si film was observed than in the usual plasma CVD. The reason is attributed to the slower deposition rate due to the small incoming fluxes, that is, surface migrations, hydrogen elimination reactions and bond formation reactions for adsorbed radicals have enough time to form tetrahedral structures before burial.

CONTROL OF REACTIVE PLASMAS FOR THE CVD

Plasma control for a-Si:H deposition in a diode type reactor

Although much empirical knowledge has been compiled for controlling the plasma for the CVD of a-Si:H in individual reactors, we need systematic guiding principles for the plasma control applicable to any reactors based on the physico-chemical processes in the plasma. From the

experimental and theoretical arguments described above we can draw a scheme as shown in Fig.9 on the relations of the external controlling parameters such as the gas pressure and flow rate, the RF input power and the dimensions of the reactor with the internal plasma parameters which govern the processes in the plasma and on the surface.

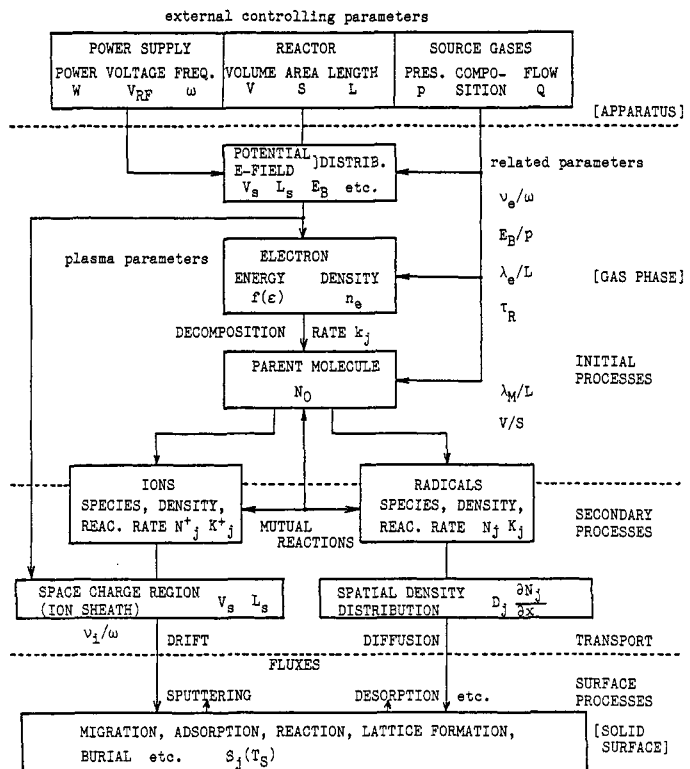

Fig.9. Schematic representation for the correlations between the external controlling parameters and the internal plasma parameters and kinetic processes.

For the control of the initial processes triggered by electron collisions, the energy and density of electrons must be controlled in the first place. Changes in the gas pressure p, the applied voltage V_{RF}, the frequency ω and the characteristic length L produce changes in the internal parameters such as ν_e/ω, E_B/p, λ_e/L, where ν_e is the electron collision frequency, E_B is the electric field strength in the bulk plasma and λ_e is the electron mean free path. In general, increases in these internal parameters lead to enhancement of the higher energy part of EEDF in the bulk plasma and in turn make changes in the rate constants for electron collision processes. However it is also important to see the division of the deposited energy between the sheath region and the bulk plasma. If we decrease p keeping V_{RF} and ω constant, the sheath voltage V_s as well as the length will increase and the energy deposition in the sheath becomes predominant. Then the discharge becomes like a hollow cathode discharge, and high energy electrons will be injected from the sheath into the plasma in comparison to the opposite case where the discharge becomes like a positive column. Similar changes will be caused when we increase V_{RF} keeping the other two parameters constant. These rough schemes conceivable from Fig.9 must be followed up quantitatively by detailed simulation as tried by Kushner (refs.8,47). It is also pointed out by Kushner (ref.8) that the presence of negative ions affects the features of the discharge.

EEDF can also be changed by using diluent gases to the source gases because the apparent cross sections can be changed for electron collisions. If EEDF is modified, the differences in the threshold energies for each electron collision processes produce changes in the initial fragmentation pattern of source gases. Other elaborate means have also been tried by many authors in order to have selected initial decomposition reactions. In an example, excited species such as the metastable rare-gas atoms (ref.62) or reactive species such as H (refs.63,64) and F (ref.64) are produced separately and transported to the place where the secondary reactions and deposition take place. In another example, though which is not categorized into the plasma CVD, the direct photodissociation or photo-sensitized reactions are utilized as the selective initial decomposition reactions.

The relative weight for the secondary gas-phase reactions can be controlled by changing the internal parameters such as λ_M/L and τ_R, where λ_M is the mean free path of radicals and τ_R is the residence time in the plasma, by changing the external parameters such as p, L and the volume to surface ratio V/S of the system. The extraction rates of ions and radicals from the plasma to the substrate change not only the surface reactions and the deposition rate but also the secondary reactions in the gas-phase because the absolute densities of ions and radicals in the plasma are determined from the balance between the production rates and the extinguishing rates. Control of the extraction rates for neutral radicals is possible through the modification of their spatial distributions.

Hirose _et al._(ref.65) modified the sheath thickness L_s by using an external inductance inserted between the substrate electrode and the ground. When the inductance was in series resonance with the sheath capacitance, L_s decreased due to the decrease in the sheath impedance and then the rate of diffusional transfer increased while the density of radicals was kept low. In this way they succeeded in the high speed deposition, suppressing the aggregat-

ing reactions in the gas-phase which deteriorate the film quality. Another way for realizing a high deposition rate is suggested from the above argument. If we decrease the electrode separation d keeping the product pd constant, we can expect the same effects as can be seen from the results of Ishihara et al.(ref.66) shown in Fig.10.

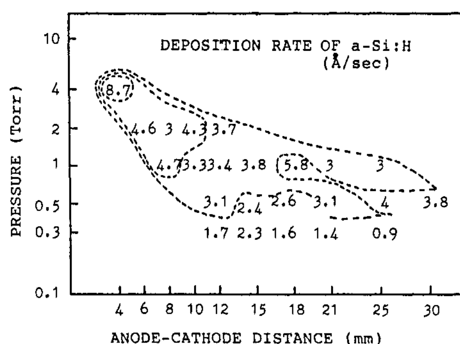

Fig.10. Measured deposition rate as functions of the pressure and the electrode distance in a 100% SiH_4 plasma at a gas flow rate of 60 standard $cm^3 min^{-1}$ and an RF power of 24 W. The electrode diameter was 30 cm (ref.66).

The surface reactions can be controlled upon a principle that the flux composition depends on the kind of source gases and the diluent gases. As can be seen from the simulation given in Fig.8 above, the expected most predominant component of the fluxes is SiH_2 for a SiH_4-Ar mixture, while the relative weights of SiH_3 and Si_nH_m(n>2) fluxes increase for other mixtures. Use of a triode type reactor (ref.67) also changes the flux composition as a function of the substrate distance from the grounded mesh electrode by decreasing λ_e/L.

The quality of the deposited film is affected more significantly by the balance between the radical transport rate and the deposition rate. Since the migration and some of the surface reactions do need activation energies, the substrate temperature T_s is an important external controlling parameter for the surface reactions. The energy of ions bombarding the substrate also contributes to the activation of surface reactions. Application of a DC bias to the substrate electrode and application of a magnetic field perpendicularly to the electrode axis are listed as some of the trials of controlling the effects of ion bombardment.

Besides the commonly used diode type RF discharge many other types of discharge such as a coaxial-line type microwave discharge (ref.68) and a microwave ECR (electron cyclotron resonance) discharge (ref.69) have been proposed recently for the CVD of a-Si:H and its compounds. Itatani et al. (ref.70) tried a PIG (Phillips Ion Gauge) type discharge which could be operated even at very low pressures. They claimed that the discharge was very effective as a method for the treatment of exhaust gases from a CVD reactor. Film deposition by this type of discharge is interesting, although the properties of deposited film have not been studied as yet.

Plasma control for the CVD of Si-compounds

For the plasma CVD of Si-compound amorphous semiconductors such as SiC, SiGe and insulators such as SiO_2 and Si_3N_4, we have to use mixtures of source gases of different physical and chemical properties. Therefore, we need more precise plasma control in order to obtain desired film compositions and electrical and optical properties. Let us take up some compounds and consider specific problems to their preparations.

For the CVD of a-Si_xC_{1-x}:H a mixture of silane gas and hydrocarbon gas is used. In general, silanes (SiH_4, Si_2H_6 etc.) are more easily decomposed by electron collisions than hydrocarbons (CH_4, C_2H_6, C_2H_4, C_2H_2 etc.). Therefore, the initial gas composition must be adjusted properly for a desired film composition. Many selections of the gas pairs have also been tried for the same purpose. From the standpoint of plasma control, the modification of EEDF for controlling the initial decomposition pattern is more interesting. This is realized, e.g., by using diluent gases (ref.71), or separating the plasma chambers for each source gases (ref.72).

In the gas-phase reactions some intercombination reactions of Si-containing radicals with hydrocarbon molecules or those of C-containing radicals with silane molecules such as listed in Table 3 may occur. But the contributions of these reactions to the decomposition of the source gas molecules are small due to the small rate constants or due to the small radical densities, although small amounts of interconnected products such as $SiCH_6$ have been detected in the plasma (ref.73). Therefore, as mentioned by Catherine (ref.73) we can imagine a scheme that each source gas is decomposed separately by electron collisions in the plasma and the produced radicals are transported separately to the substrate, where the compound

TABLE 3. Examples of the intercombination gas-phase reactions and the parameters A and E for the rate constants given by K = A exp(-E/RT) as in Table 2.

Reactions	A	E/R
$CH_2 + SiH_4 \rightarrow CH_3SiH_3$	1.4(14)	0
$SiH_2 + CH_4 \rightarrow CH_3SiH_3$	6.0(11)	0
$CH_3 + SiH_4 \rightarrow CH_4 + SiH_3$	7.8(11)	3490
$C_2H_5 + SiH_4 \rightarrow C_2H_6 + SiH_3$	5.4(11)	3620
$CH_3 + Si_2H_6 \rightarrow CH_4 + Si_2H_5$	7.9(11)	2780
$C_2H_5 + Si_2H_6 \rightarrow C_2H_6 + Si_2H_5$	5.6(11)	2830

film is deposited via surface reactions.

The difference in the reactivities for C-containing radicals and for Si-containing radicals, however, causes degradations of the film properties. Matsuda et al.(ref.74) assumed that CH_n (n = 0-3) radicals tend to abstract surface bonded H atoms and lower the hydrogen coverage of growing surface. This causes a large number of defects left in the film. Under this assumption they tried to dilute the gas mixture with hydrogen for a compensation of the hydrogen coverage by expecting an enhanced H-atom flux, and obtained a film of fairly high photoconductivity.

For the CVD of a-Si_xGe_{1-x}:H the situation reverses; GeH_4 is more easily decomposed than SiH_4. For the control of the decomposition pattern some method for decreasing the higher energy tail of EEDF must be considered. Intercombination reactions in the gas-phase in this system also seem to be negligible. But other problems arise due to the small diffusibility and high reactivity of Ge-containing radicals GeH_n (n<2) on the growing surface. Matsuda et al.(ref.74) tried to eliminate those radicals and enhance GeH_3 by using a triode type reactor, and succeeded in preparing fairly good quality films.

In plasmas for the preparation of insulator films such as SiO_2 and Si_3N_4, gas mixtures of silane with N_2O, O_2, NH_3, N_2 and so on are used, where intercombination reactions must be more significant. Therefore, these systems are more interesting from a viewpoint of the gas-phase reaction modeling. Plasma simulations for these systems remain as future problems.

CONCLUDING REMARKS

In this talk the present status of the activities of Plasma Electronics Society in Japan in the field of diagnostics and control of CVD plasmas has been reviewed with some complementary introduction of advanced studies in other countries. The diagnostics of the processing plasmas has been tackled both theoretically and experimentally, and some guiding principles for the control of the plasmas have become clear. However, the results are far from satisfaction at present because of the lack in the basic data compilation for the reaction kinetics, the crude approximations in the simulation, the poor experimental diagnostics, especially, on the densities of important radicals, the sheath structures and the electric field strength in the plasma. This situation motivated us to organize a project study on "Control of Reactive Plasmas" conducted by Prof. Itatani of Kyoto University under the support of a Grant-in-Aid for Science Research on Priority Areas from Japanese Ministry of Education, Science and Culture for three years starting from 1988.

REFERENCES

1. D.B. Graves and K.F. Jensen, IEEE Trans. Plasma Sci. PS-14, 78 (1986).
2. K. Suzuki, K. Ninomiya, S. Nishimatsu, J.W. Thoman Jr. and J.I. Steinfeld, Jpn. J. Appl. Phys. 25, 1569 (1986).
3. A. Metze, D.W. Ernie and H.J. Oskam, J. Appl. Phys. 60, 3081 (1986).
4. A.M. Pointu, Appl. Phys. Lett. 50, 316 (1987).
5. H. Shimabukuro, Y. Ichikawa, H. Sakai and Y. Uchida, Proc. 4th Symp. Plasma Processing (Yokohama, 1987) p.182.
6. K. Kitamori, M. Shimozuma and H. Tagashira, ibid, p.169.
7. M.J. Kushner, J. Appl. Phys. 54, 4958 (1983).
8. M.J. Kushner, IEEE Trans. Plasma Sci. PS-14, 188 (1986).
9. T. Makabe, Proc. 7th Int. Symp. Plasma Chemistry (Eindhoven, 1985) p.1331.
10. H. Mase, T. Tanabe and T. Ikehata, Proc. 3rd Symp. Plasma Processing (Kiryu, 1986) p.135.
11. R. Itatani, Proc. 4th Symp. Plasma Processing (Yokohama, 1987) p.178.
12. I. Ishikawa, S. Suganomata and M. Matsumoto, Proc. 3rd Symp. Plasma Processing (Kiryu, 1986) p.170.
13. S. Matsumura, 4th Symp. Plasma Processing (Yokohama, 1987) p.44.
14. H. Amemiya, ibid, p.66.
15. T. Akitsu, ibid, p.57.
16. M. Sugawara and J. Ichihashi, Proc. 3rd Symp. Plasma Processing (Kiryu, 1986) p.140.
17. K. Kato, R. Hatakeyama, N. Sato and Y. Nakagawa, ibid, p.6.
18. A. Boschi et al., Nuovo Cimento, 29, 487 (1963).
19. C.A. Moore, G.P. Davis and R.A. Gottsho, Phys. Rev. Lett. 52, 538 (1984).
20. K. Kawasaki, T. Usui and T. Oda, J. Phys. Soc. Jpn, 51, 3666 (1982).
21. T. Sato and T. Goto, Jpn. J. Appl. Phys. 25, 937 (1986).
22. T. Sato, F. Shibata and T. Goto, Chem. Phys. 108, 147 (1986).
23. K. Tint, A. Kono and T. Goto, Proc. 8th Int. Symp. Plasma Chemistry (Tokyo, 1987) (to be published).
24. T. Sato, A. Kono and T. Goto, Proc. 4th Symp. Plasma Processing (Yokohama, 1987) p.239.
25. Y. Ohmori, M. Shimozuma and H. Tagashira, J. Phys. D, 19, 1029 (1986).
26. Y. Ohmori, K.Kitamori, M.Shimozuma and H.Tagashira, ibid, 19, 437 (1986).
27. K. Tachibana, M.Nishida, H.Harima and Y.Urano, J. Phys. D, 17, 1727(1984).

28. K. Tachibana, T. Okuyama, H. Harima and Y. Urano, Proc. 7th Int. Symp. Plasma Chemistry (Eindhoven, 1985) p.588.
29. N. Hata, Proc. 3rd Symp. Plasma Processing (Kiryu, 1986) p.201.
30. N. Hata and K. Tanaka, J. Non-Cryst. Solids, 77&78, 777 (1985).
31. K. Tachibana, H.Tadokoro, H.Harima and Y.Urano, J. Phys. D, 15, 177(1982).
32. Y. Takubo and M. Yamamoto, Proc. 4th Symp. Plasma Processing (Yokohama, 1987) p.197.
33. G. Inoue and M. Suzuki, Chem. Phys. Lett. 105, 641 (1984).
34. G. Inoue and M. Suzuki, Chem. Phys. Lett. 122, 361 (1985).
35. T. Amano, P.F. Bernath, C. Yamada, Y. Endo and E. Hirota, J. Chem. Phys, 77, 5284 (1982).
36. C. Yamada and E. Hirota, Phys. Rev. Lett. 56, 923 (1986).
37. Y. Matsumi, S. Gohe, T. Hayashi and M. Komiya, Proc. 3rd Symp. Plasma Processing (Kiryu, 1986) p.24; J. Vac. Sci. Technol. A4, 1786 (1986).
38. G. Turban, Y. Catherine and B. Grolleau, Thin Solid Films, 67, 309 (1980).
39. J. Perrin, A. Lloret, G.de Rosny and J.P.M. Schmitt, Int. J. Mass Spectrom. Ion Phys. 57, 249 (1984).
40. R.Robertson and A.Gallagher, J. Appl.Phys. 59,3402(1986); Appl. Phys. Lett. 43,544(1983).
41. J.W. Hudgens, T.G. DiGiuseppe and M.C. Lin, J. Chem. Phys. 79, 571 (1983).
42. J.Berkowitz, J.P.Greene, H.Cho and B.Ruscic, J. Chem.Phys. 86, 1235(1987).
43. K. Tachibana, Proc. 8th Symp. Ion Sources and Ion Assisted Technology (Tokyo, 1984)p.319.
44. A. Yuuki, Y. Matsui and K. Tachibana, Jpn. J. Appl. Phys. 26, 747 (1987).
45. Y. Matsui, A.Yuuki, N.Morita and K.Tachibana, Jpn.J.Appl.Phys.26,(1987)(to be published).
46. L.E. Kline, W.D.Partlow and W.E.Bies, Proc.Electrochem.Soc.Symp.Plasma Processing (1986).
47. M.J. Kushner, MRS Symp. Proc. Vol.68, Plasma Processing, p.293 (1986).
48. A. Sumiyama, Y. Yamaguchi and T. Makabe, Proc. 4th Symp. Plasma Processing (Yokohama, 1987) p.321.
49. A. Gallagher, J. Appl. Phys. 60, 1369 (1986).
50. G. S. Selwyn, J. Appl. Phys. 60, 2771 (1986).
51. J.P.M. Schmitt, J. Non-Cryst. Solids, 59&60, 652 (1983).
52. J. Perrin and T. Broekhuizen, Appl. Phys. Lett. 50, 433 (1987).
53. K. Muraoka et al. Proc. 4th Symp. Plasma Processing (Yokohama, 1987) p.88.
54. F.J. Kampas and R.W. Griffith, Appl. Phys. Lett. 39, 407 (1981).
55. M. Hirose, Jpn. J. Appl. Phys. 21, Suppl.21-1, 275 (1982).
56. A. Gallagher, MRS Symp. Proc. Vol.70, Materials Issues in Amorphous Semiconductor Technology, p.3 (1986).
57. M. Tsuda, M. Nakajima and S. Oikawa, J. Am. Chem. Soc. 108, 5780 (1986).
58. A. Matsuda, J. Non-Cryst. Solids 59&60, 767 (1983).
59. H. Sugai, H. Toyoda, T. Okuda and A. Yoshida, Proc. 4th Symp. Plasm Processing (Yokohama, 1987) p.317; Appl. Phys. Lett. 48, 1648 (1986).
60. H. Tagashira et al. Proc. 3rd Symp. Plasma Processing (Kiryu, 1986) p.69.
61. S. Miyazaki, H. Hirata, S. Ohkawa and M. Hirose, J. Non-Cryst. Solids 77&78, 781 (1985).
62. Y. Toyoshima et al. Appl. Phys. Lett. 46, 584 (1985).
63. Y. Toyoshima et al. Proc. 3rd Symp. Plasma Processing (Kiryu, 1986) p.73.
64. J. Hanna, and OI. Shimizu, Proc. 4th Symp. Plasma Processing (Yokohama, 1987) p.139.
65. T. Hamasaki, M.Ueda, A.Chayahara, M.Hirose and Y.Osaka, Appl. Phys. Lett. 44, 1049(1984).
66. S. Ishihara and T. Hirao, Proc. 46th Annual Meeting of Jpn. Soc. Appl. Phys. Soc. (Kyoto, 1985) p.748.
67. A. Matsuda and K. Tanaka, J. Appl. Phys. 60, 2351 (1986).
68. O. Kato, S. Wakata and S. Hata, Jpn. J. Appl. Phys. 22, L40 (1983).
69. S. Matsuo et al. Jpn. J. Appl. Phys. 22, L210 (1983).
70. R. Itatani et al. Proc. 4th Symp. Plasma Processing (Yokohama, 1987) p.29.
71. K. Tachibana , H. Harima and Y. Urano, Proc. 8th Int. Symp. Plasma Chemistry (Tokyo, 1987) (to be published).
72. M. Motohashi et al. Proc. 34th Joint Meeting of Jpn. Soc. Appl. Phys.(Tokyo, 1987) p.228.
73. Y. Catherine, G. Turban and B. Grolleau, Thin Solid Films, 76, 23 (1981).
74. A. Matsuda, Proc. 4th Symp. Plasma Processing (Yokohama, 1987) p.164; Proc. 8th Int. Symp. Plasma Chemistry (Tokyo, 1987)(to be published).